JOURNAL OF AIRCRAFT
Vol. 48, No. 4, July–August 2011

Fatigue Crack Initiation and Propagation in Aileron Lever Using Successive-Initiation Modeling Approach

James Gyllenskog*
U.S. Air Force, Hill Air Force Base, Utah 84056
and
Leila J. Ladani†
University of Alabama, Tuscaloosa, Alabama 35487

DOI: 10.2514/1.C031297

Crack initiation and propagation due to cyclic mechanical fatigue damage in the T-38 aileron lever is modeled using a continuum damage modeling approach in conjunction with a "successive-initiation" technique. Successive initiation is a continuum-based damage-propagation methodology that is based on updating the state of damage in material and accumulating damage in individual elements according to their stress-life history. The elements are eliminated from the structure if they exceed the defined damage threshold. In contrast to available fracture-mechanics approaches, this method does not require an initial crack and is capable of determining the initiation site. The model is used to predict the number of cycles to crack initiation and propagation to critical size. This approach successfully predicts the location of crack initiation, propagation path and propagation rate. Field data and experimental observations of the cracks correlated very well with finite element results. Probability design approach using a Monte Carlo simulation is used to determine the sensitivity of fatigue-life response to variation in load and mechanical-property inputs. As expected, the most important parameter was found to be the damage exponent. A sensitivity study was conducted without damage parameters as input variables. The results of this study show that load variations are more important than material-property variations.

Nomenclature

b	=	fatigue strength exponent
c	=	fatigue ductility exponent
D	=	damage
D_{accum}	=	accumulated damage
D_c	=	damage per cycle
D_{ci}	=	damage per incremental cycle
E	=	Young's modulus
$\tilde{E}$	=	effective Young's modulus
N_i	=	incremental number of cycles applied
N_f	=	number of cycles to failure
N_{fi}	=	number of cycles for incremental propagation of damage
N_1	=	number of cycles to initiate crack
ε_p	=	plastic strain
ε'_f	=	fatigue ductility coefficient
$\tilde{\sigma}$	=	effective stress
σ_a	=	stress amplitude
σ'_f	=	fatigue strength coefficient

I. Introduction

THE aileron lever is a critical single-point failure item for the T-38 flight control system. Stick inputs from the pilot are transferred through the lever arm to the servo valve, which moves the ailerons up or down during flight in relation to stick movements (Fig. 1). If the lever arm were to break in flight, uncommanded rolling of the aircraft would occur. In critical situations such as takeoff and landing with little time to recover, uncommanded rolling could result in loss or substantial damage to the airframe or death or serious injury to the flight crew. Based upon these scenarios, the aileron lever arm is identified as a critical safety item.

Following a 2008 mishap of a T-38 aircraft that resulted in loss of lives of two pilots, a comprehensive investigation was conducted to identify the cause. Clear and convincing evidence showed that the aileron lever had failed in fatigue before aircraft takeoff. This investigation led to two separate studies in an effort to determine the fatigue life of the lever.

Immediately following the investigation, Southwest Research Institute (SwRI) was contracted by Hill Air Force Base to perform an analysis of the lever for two purposes: first, to determine what kind of loading the aileron lever was experiencing; second, to determine the replacement and inspection interval that should be followed. The SwRI study [1] determined that the maximum and minimum loads experienced by the lever were 92.45 and −105.19 lb, respectively. This was determined by applying several strain gauges to the lever with hydraulic power applied to the aircraft, having pilots simulate control-stick movements as they would while in flight. The SwRI analysis resulted in a recommendation to replace the lever every 900 h.

The study conducted by SwRI, followed a classical fracture-mechanics analysis of the lever using the computer software AFGROW. The SwRI study focused solely on the location of the crack that caused the mishap. This, however, contradicted the vast field data available. A study of 275 parts performed by the Materials Laboratory at Hill Air Force Base showed that 127 were cracked in one location, 74 were cracked in multiple locations, and 74 parts had no evidence of any cracks. Of the parts studied, only one lever showed evidence of cracking in the location on which SwRI focused their study. This anomaly led to the conclusion that the mishap lever had a manufacturing defect in the location of the crack. The defect served as a stress riser, resulting in more damage occurring in that area than was predicted by the finite element model. Their study, however, was unable to determine the crack initiation site and propagation path that naturally occurs due to fatigue damage accumulation. The goal of this study was to fill this gap.

For the past several decades, various damage models derived from continuum damage mechanics (CDM) center on the microvoid/crack development and provide an understanding of the mechanics of fracture in structures by means of damage variables that represent the deterioration of a material element [1–6].

Received 5 November 2010; revision received 15 December 2010; accepted for publication 15 December 2010.

*T-38 Aircraft Structural Integrity Branch; james.gyllenskog@hill.af.mil.
†Mechanical Engineering; lladani@eng.ua.edu (Corresponding Author).

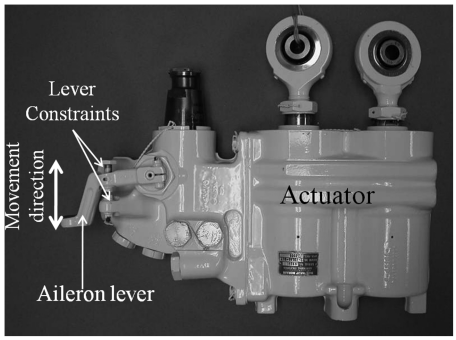

Fig. 1 Aileron actuator assembly.

Introduced by Kachanov in 1958 [7], continuous damage mechanics was originally used to model creep rupture, but has since been developed for use in modeling low cycle fatigue, high cycle fatigue, coupling between damage and cyclic creep, and creep/fatigue interaction [3]. Lemaitre [3] also indicated that this area of solid mechanics is based on metallurgy and provides a better understanding of rupture in structures by defining a variable that represents the deterioration of the material before the initiation of a macrocrack.

Chaboche [4] described CDM as a tool to describe phenomena before crack initiation. According to Chaboche, CDM is based on the framework of irreversible processes and offers complementary possibilities to linear elastic fracture mechanics [4]. The final state of CDM generally corresponds to the presence of a material discontinuity, crack initiation, which is sufficiently large compared with the grains and subgrains. The theory of CDM is supported by the physical idea that before crack initiation, a progressive internal deterioration of the material occurs [4]. There are several methods that can be used when measuring the damage sustained during loading. Along with density changes, or electric resistivity measurements, there are measures of remaining life that are typically used in creep and fatigue, measures in the reduction of fatigue limits that require numerous tests to define damage evolution curves, and measures of the stress–strain behavior.

In a two-part paper, Chaboche [5,6] presented the general concepts of CDM, which are damage growth, crack initiation, and crack growth. According to Chaboche [6], "the damaging process corresponds to localizations and accumulations of the strains and are considerably more irreversible." Defects in materials lead to progressive material deterioration (material damage), crack initiation, and finally fracture. These effects can be measured through the decrease in stiffness, the toughness, the strength, and the residual life of the material after damage has accumulated.

Crack initiation is defined by Chaboche [6] as the "breaking up" of a continuum volume element. Just like fracture mechanics, the objective of damage theory is to predict the life of a structure. Being able to accurately predict the life of a structure is of utmost importance for design engineers.

A major concept that comes from damage theory is that of remaining life. Remaining life is best described as N/N_f, where N and N_f represent the current number of cycles already applied and the number of cycles to failure, respectively. The concept of remaining life can best be illustrated in Eq. (1), where D is the damage after the initial damaging process. The damage constant D will be equal to 0 for the undamaged material and 1 at the time of rupture. After the initial period, the damage accrued is

$$D = \frac{N_1}{N_{F1}} \tag{1}$$

where N_1 is the number of cycles that has been applied to the material at a stress amplitude σ_a, and N_{F1} is the number of cycles to failure at the same stress amplitude. The remaining life of the material after the initial damage period is shown in Eq. (2):

$$\frac{N_2}{N_{F2}} = 1 - D \tag{2}$$

Fatigue does not have a unique damage evolution curve as a function of the life ratio N/N_f. Instead, it is dependent on the applied load and the state of damage itself. In other words, as the material is damaged its constitutive properties change and it accumulates damage with a different rate.

Both Lemaitre [2,3] and Chaboche [4–6] described damage measures using the effective-stress concept. The notion behind the effective stress is that a damaged material under an applied stress σ shows the same strain response as the undamaged material under the effective stress. Using damage D to represent the loss of effective area, the effective stress can be seen in Eq. (3):

$$\tilde{\sigma} = \frac{\sigma}{1 - D} \tag{3}$$

Lemaitre [2,3] takes the damage variable D one step further by applying the effective-stress concept to the elasticity modulus in Eq. (4). Using Young's modulus E, the elasticity modulus of the damage material could be considered as

$$\tilde{E} = E(1 - D) \tag{4}$$

With the variable E being known, $\tilde{E}$ can be measured through tension tests. CDM has been shown to be an exceptionally useful tool.

The current study is also based on effective stress and uses finite element analysis to find the effective stress in the material as a crack propagates due to fatigue. A successive-initiation technique is used in conjunction with a stress-based continuum damage model to predict the fatigue crack initiation site and propagation path. The continuum damage model used is able to successfully predict the locations where cracks are most likely to occur without any presumptions being made.

II. Continuum Damage Models

Several models have been proposed to determine the number of cycles to failure based on stress, strain, or energy. The stress-based approach to life prediction is the oldest method used in fatigue modeling [8]. In this method, the fatigue life of a material is expressed as a function of a strength parameter. Basquin [9] proposed the equation

$$\sigma_a = \sigma'_f (2N_f)^b \tag{5}$$

where σ_a is the stress amplitude, σ'_f is called the fatigue strength coefficient, and b is the fatigue strength exponent. Power-law equations are the most common type equations for stress-based fatigue-life models.

The strain-based approach to fatigue modeling is one of the most widely used approaches for predicting the life of a material and is especially useful in the case of low cycle fatigue. If only plastic strain is considered, the function that correlates the number of cycles to plastic strain is the widely used Coffin–Manson [10,11] equation and is as follows:

$$\frac{\Delta\varepsilon_p}{2} = \varepsilon'_f (2N_f)^c \tag{6}$$

where ε'_f is the fatigue ductility coefficient, c is the fatigue ductility exponent, and $\Delta\varepsilon_p$ is the inelastic strain range in one cycle.

A. Damage Model

To predict crack initiation and propagation using finite element analysis, a damage model is required. The initial material used for the lever is aluminum 2014-T6. After the mishap, however, all the old levers were replaced by a material that could be easily manufactured, and all the old levers were removed for inspection. The fatigue analysis is conducted for both the main material and the alternate material: aluminum 7050-T74.

Based on the literature search, the only available damage model with the required damage constants for 2014-T6 aluminum is a

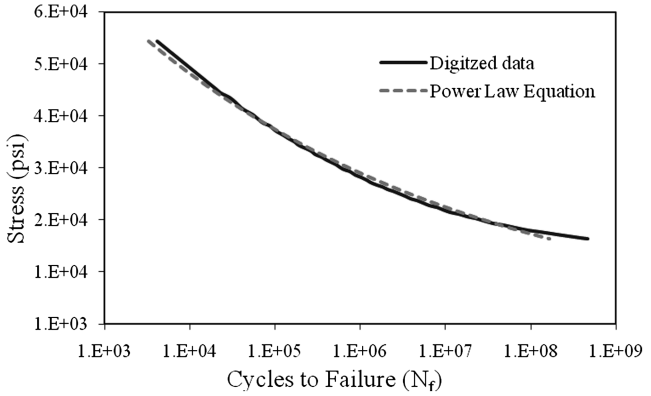

Fig. 2 *S–N* curve for 2014-T6 comparing original digital data with the equation found from a power-law fit.

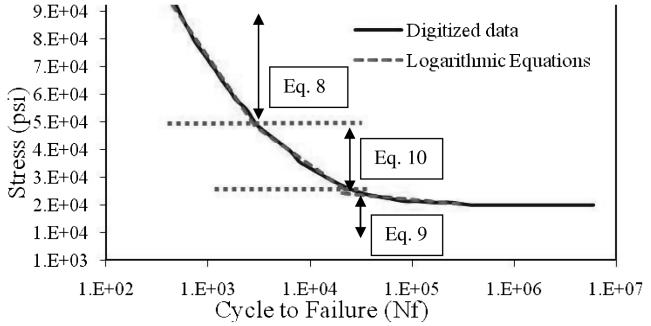

Fig. 3 *S–N* curve for 7050-T74 comparing original digital data with the equation found from exponential fit.

stress-based damage model developed by Hayden et al. [12]. Beginning with the *S–N* curve for 2014-T6 aluminum, digital software was used to retrieve data points and create a plot. A power-law curve was fit to the data in order to obtain the equation of the line. Solving for the number of cycles to failure, N_f, gave Eq. (6). Figure 2 depicts the original *S–N* curve used to calculate the damage constants, along with the plot of Eq. (7) using the same stress amplitudes as the original curve for the aluminum material:

$$N_f = C(\sigma_a)^m \tag{7}$$

where σ_a is the stress amplitude and C and m are material damage constants calculated as 6.2874E + 47 and −9.33707, respectively.

Using a similar technique, but employing logarithmic functions and Fig. 3 three individual curves were used to calculate the damage constants of the alternate 7050-T74 material at different stress ranges. This provided an additional challenge in the ANSYS code to select the proper damage constants depending on the stress. The equations used can be seen in Eqs. (8–10):

$$N_f = \exp\left(\frac{-(\sigma_a - 237090)}{23540}\right) \tag{8}$$

$$N_f = \exp\left(-5 \cdot \frac{-(\sigma_a - 39965)}{7423}\right) \tag{9}$$

$$N_f = \exp\left(\frac{-(\sigma_a - 139931)}{11351}\right) \tag{10}$$

Equation (8) was used to calculate N_f for any element with a stress greater than or equal to 50,000 psi. Similarly Eq. (9) was used to calculate N_f for any element with a stress less than 26,000 psi. And finally, Eq. (10) was used to calculate N_f for any element with a stress between 26,000 and 50,000 psi. A constant-amplitude loading cycle was used for this investigation to mimic worst-case scenario on the lever. Using slightly lower values that those found in the SwRI study, the maximum and minimum loads applied to the lever were 83.25 and −93.7 lb. The loads were lowered to allow for the probability analysis to have mean values of 92.45 and −105.19 with a ±10% standard deviation.

III. Finite Element Simulation

Using ANSYS, a three-dimensional finite element model was built to calculate stresses on individual elements with a known applied load. The ANSYS code was written in such a way that it would conduct the modeling, meshing, applications of boundary conditions and loads and solutions automatically for many runs and predict the location of the cracks and the number of cycles to grow a crack to a critical length. Figure 4 shows a 3-D image of the solid model drawn in ANSYS. The mechanical properties used in the analysis are shown in Table 1.

A. Mesh

A SOLID186 element was chosen from the ANSYS library to use in the meshing sequence. A SOLID186 is a higher-order 3-D 20-node element that exhibits quadratic displacement behavior. Each node has three degrees of freedom: translation in the x, y, and z directions [13]. This element is well suited to meshing the irregular shapes created in modern CAD systems. Figure 4 shows the mesh. A total of 53,422 elements were created. The ability to mesh irregular shapes was necessary for this model because of the curved surfaces around the center of the lever. A finer mesh was applied to the areas of most interest and where stresses were assumed to be the highest.

B. Boundary Conditions and Loading

The upper and lower surfaces of the lever shown in Fig. 4 are constrained by the upper and lower constraints shown in Fig. 1. Therefore, the same constraints were applied to two different locations on the model. Figure 5 shows the locations where the constraints were applied. Figure 5a shows the location where the lever attaches to the servo valve. Figures 5b and 5c show the constraints applied on the lower and upper surfaces, respectively, while the load is applied.

In Fig. 5a, constraints were applied to individual nodes restricting the model from translating in the x, y, and z directions (see the coordinate system shown in Fig. 4). The constraints in Figs. 5b and 5c were applied to lines around the center bore of the lever simulating the bolt head and nut that prevent the lever from overtravel and constraining the motion in the positive and negative z directions only.

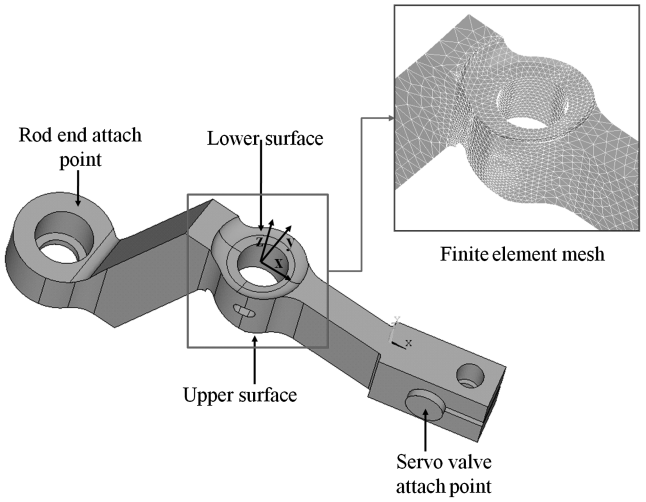

Fig. 4 Three-dimensional model built in ANSYS and finite element mesh.

Table 1 Mechanical properties used in finite element analysis for two types of aluminum

Aluminum	E, ksi	Yield strength, ksi	Ultimate strength, ksi	υ
7050-T74	10400	68	76	0.33
2014-T6	10500	60	70	0.33

Cyclic loading using the maximum and minimum loads discussed previously was used to calculate the fatigue life of the lever. A load of 83.25 lb was uniformly distributed to the nodes on the rod end of the lever in the positive z direction, as shown in Fig. 6a. This configuration created compressive and tensile stresses on the lower and upper surfaces of the lever, respectively. Loading of the lever while on the aircraft only happens for a brief second when full stick deflection is applied by the pilot. All loads and constraints were removed from the model and reapplied in a similar configuration with the differences being the upper surface was constrained from moving in the z direction, and a load of 93.7 lb was uniformly distributed to the nodes in the negative z direction, as shown in Fig. 5b. This configuration created compressive and tensile stresses on the upper and lower surfaces of the lever, respectively. Again, the load was applied for a time of 1 s and then released. Figure 7 is a graph of the cyclic loading depicting the maximum and minimum forces. During each time step, the equivalent stresses for individual elements were calculated and stored. Using `ETABLE` commands in ANSYS allows for the calculated stresses to be operated on as necessary.

IV. Successive Initiation

Successive initiation was first introduced by Okura [14] and later used to determine the crack initiation and propagation site and rate in elastic–plastic–viscoplastic materials [15–17]. The results have been correlated with experiments and this method has shown strong promise in detecting the crack initiation site and propagation path. This finite element method can be used with any damage model to simulate fatigue crack initiation and propagation in materials. The successive-initiation analysis requires several steps of finite element. The flowchart of the successive-initiation process can be seen in Fig. 8 with a description of the process following.

Beginning with the stress-based model discussed previously, the damage initiation site was first identified using constant-amplitude cyclic loading. A set of finite elements surrounding the initiation site with damage above a selected threshold were identified as the damage initiation zone. These elements were "killed" in ANSYS, which resulted in the elements no longer adding to the stiffness matrix of the solution.

As the load cycle is applied on the lever, the stress amplitude varies throughout the finite element model. As expected, some elements have higher stress amplitudes, resulting in a higher damage-accumulation rate. Initially, the stress amplitude for each element was calculated. Using Eqs. (7–10), the number of cycles to failure, N_f, was calculated for each individual element. Assuming the elements accumulate damage with a constant rate (or, in other words, damage accumulated in each cycle is equal) and that maximum

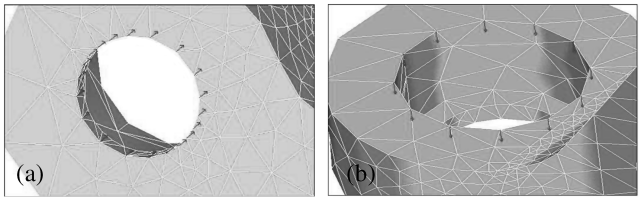

Fig. 6 View of applied loads on lever: a) 83.25 lb load being applied in the positive z direction and b) 93.7 lb load being applied in the negative z direction.

damage accumulation is 1, the damage per cycle can be calculated using the following equation:

$$D_c = \frac{1}{N_f} \tag{11}$$

After the damage per cycle was calculated, the table was sorted from maximum to minimum damage per cycle. To initiate a crack, a criteria is set such that at least a few elements are eliminated from the structure. Therefore, using the maximum damage value, the limiting damage was determined from the following equation:

$$\lim \mathrm{d}mg = 0.05 \cdot \max \mathrm{d}mg \tag{12}$$

Several limiting damage values were tested. The limiting value used in Eq. (12) was determined to be acceptable. This limiting damage value allowed for a large enough group of elements to be selected to initiate a crack. Using the limiting damage as calculated above, any element with damage greater than the limiting damage was selected and killed. In ANSYS, when an element is killed, the element remains in the model, but does not add any stiffness to the overall stiffness matrix. This will result in the stresses of the subsequent runs to be distributed to the remaining elements surrounding the killed element. The elements that were selected and killed each have

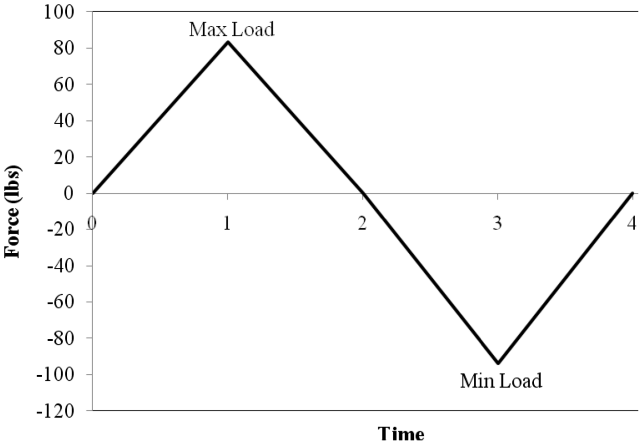

Fig. 7 Graph of cyclic loading depicting the maximum and minimum forces.

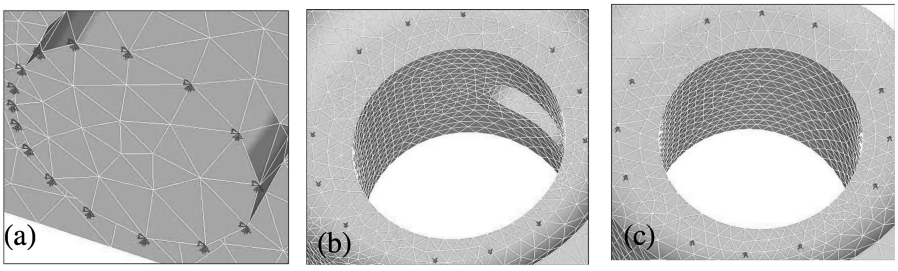

Fig. 5 View of constraints applied: a) splined end of lever is constrained from translating in x, y, and z directions, b) lower surface constrained from z displacement during positive z direction loading, and c) upper surface constrained from z displacement during negative z direction loading.

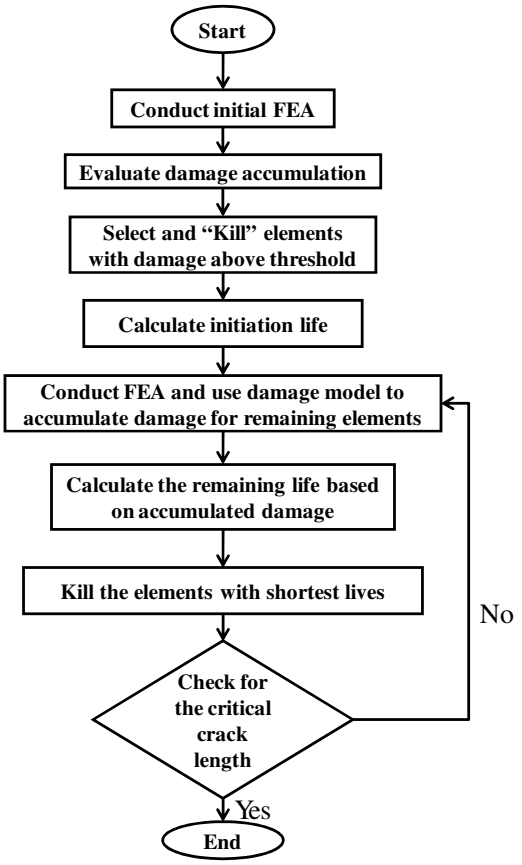

Fig. 8 Damage initiation and propagation using successive initiation (FEA indicates finite element analysis).

different fatigue lives. An averaging scheme was used to determine the initiation life using the following equation:

$$N_1 = 1 \Big/ \frac{D_{\text{summ}}}{N_e} \tag{13}$$

where D_{summ} is the summation of D_c and N_e is the total number of elements selected using the limiting damage criteria. For successive runs, the average life of each run was calculated in an identical fashion as the initiation. At the conclusion of the program, the total life of the lever was calculated by the sum of the initiation life and subsequent step lives.

In the next step, the accumulated damage was calculated using Eq. (11), where N_1 is the number of cycles completed. N_1 is the number of cycles for initiation. This value is substituted with the corresponding number of cycles in each subsequent step:

$$D_{\text{accum}} = N_1 \cdot D_c \tag{14}$$

Assuming that each element can have maximum damage of 1, using the accumulated damage found in Eq. (10), the residual damage D_r is calculated using Eq. (12):

$$D_r = 1 - D_{\text{accum}} \tag{15}$$

The calculated values of the accumulated and residual damages were stored in vector arrays to be used in subsequent runs. Once the damage values were saved, the process was repeated for a total number of 10 successive runs. The cycles to failure for the subsequent runs were calculated using

$$N_i = \frac{D_r}{D_{c_i}} \tag{16}$$

where $i = 1, 2, \ldots, 10$. The selection criterion for the remainder of the program was slightly different than the initiation run. After the completion of each successive run, the values for the accumulated and residual damages were updated and saved in place of the old data. After each successive run, the element tables were sorted by N_i and elements with extremely short lives were killed.

Two factors affect the length of the process and computation steps, first is the number of elements that are killed in each step and second is the critical crack length. There is a tradeoff between the number of runs and accurate prediction of number of cycles to crack propagation. The smaller the steps, the more accurate the crack path determination. The initiation life and the cumulative average life of the successive runs are finally combined to give the total cycles to failure.

V. Finite Element Results

The statistical data collected in the field showed that a significant number of cracks occurred in locations other than where SwRI performed their analysis. SwRI used a fracture-mechanics-based approach in which a presumption of a precrack or flaw in the material is necessary. The fracture-mechanics approach is not capable of determining the crack initiation site. Therefore, a different modeling approach in this current study is conducted to predict crack sites more accurately without presumptions and guesses and to compare the results to the field data available.

Figure 9 shows a view looking down on the upper surface of the aileron lever depicting the time designations that will be referred to throughout the remainder of this study.

After the simulations were performed in ANSYS, plots were created showing the locations and propagation paths of the cracks for 2014-T6. The alternate material showed a very rapid deterioration due to fatigue, which was also confirmed by the SwRI. So the levers made by that material were quickly removed from the field. Here, the results observed in 2014-T6 are presented. Figure 10 shows the top view and side view of the lever depicting the crack propagation path beginning with the undamaged state and ending with a complete crack connecting the 11 and 1 o'clock positions. The crack depth can also be observed in these figures. The crack depth is definitely more significant in the 1 and 11 o'clock locations.

It can be seen in Fig. 10 that the crack locations occur at the 11 and 1 o'clock positions. During the cyclic loading, a majority of the damage happens at various positions between the crack initiation sites due in part to the large compressive stresses occurring from the physical constraints placed on the lever. These data show very good agreement with the data provided from the Hill Air Force Base Materials Laboratory discussed in the following section.

To calculate the number of cycles to grow a crack to a similar length as the mishap crack, a built in function in ANSYS was used. ANSYS has the ability to measure the distance between nodal points. Using this ability was a straightforward approach to figuring out how

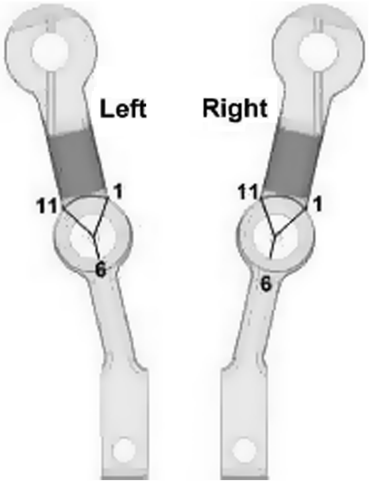

Fig. 9 View looking down on upper surface of aileron levers (courtesy of SWRI).

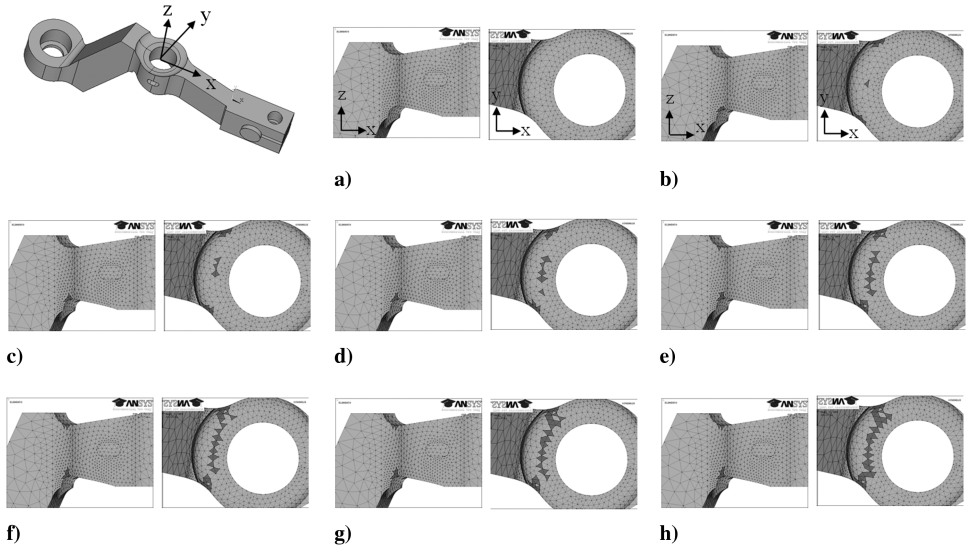

Fig. 10 Crack initiation and propagation on the upper surface of the aileron lever. The dark elements represent the killed elements during each successive sequence of the ANSYS code. Successive runs appear from left to right.

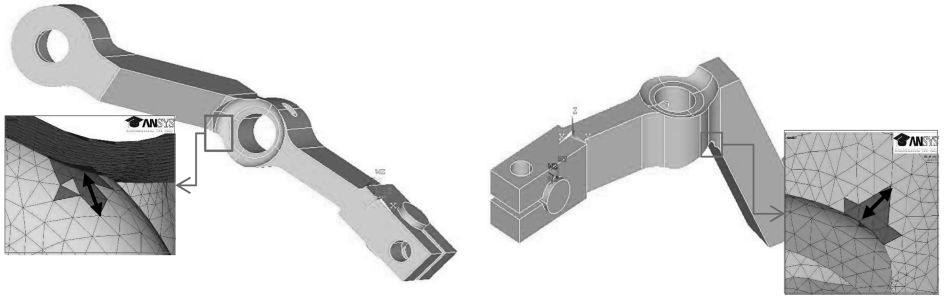

Fig. 11 Illustrations of critical crack length of a) 0.06408 in. measured between nodal points on the upper surface after a total of 208,135 cycles and b) 0.06304 in. measured between nodal points on the side after a total of 208,135 cycles.

long the cracks were and how much they had propagated between cycles. Figure 11 shows the location and length of the cracks as measured between nodal points on the upper surface and side of the lever, respectively. The lengths depicted in were established to be critical based on the length of crack that caused the original mishap. The successive-initiation technique outlined above was used to calculate the total number of cycles to grow a crack to the lengths shown in Fig. 11. A total fatigue life for the aileron lever was calculated to be 208,135 cycles. The number of cycles required to initiate a crack was 36,630.

In addition to the location and propagation paths, the propagation rate was calculated. This was again done using the built in tools in ANSYS. A length of crack was measured after the initiation cycle. The two most extreme nodal points at the 11 o'clock position on both the upper surface and the side of the lever were selected. These values were found to be 0.03922 and 0.03784 in., respectively. Figures 11a and 11b show the measurements at the final critical crack lengths. These measurements along the upper surface and side were taken after 171,505 additional cycles. The final critical crack lengths were measured at 0.06408 in. on the upper surface and 0.06304 in. along the side. The crack propagation rates were calculated using Eq. (14), where a_i is the crack length after initiation, a_f is the final crack length, and ΔN is the number of cycles required to go from the initial crack length to the final crack length:

$$\frac{\mathrm{d}a}{\mathrm{d}N} = \frac{a_f - a_i}{\Delta N} \tag{17}$$

Using this formula, the maximum crack propagation rate was calculated as 1.4693×10^{-7} in./cycle.

VI. Sensitivity Analysis

The Monte Carlo simulation was used in this study to observe the effects variability of select parameters had on the initiation life of the lever. These parameters consist of the damage constants as found using the *S–N* curve for the materials [C and m in Eq. (7)], the material properties such as the modulus of elasticity E, and the maximum and minimum loads applied to the lever ($F_{\max,} F_{\min}$). ANSYS probability design feature is used to conduct sensitivity analysis. This analysis requires probability distribution for random input parameters.

A. Random Input Values

The probability distributions of the input values must be known to input into ANSYS. One way of obtaining the probability distribution is to perform real experiments and record the scatter in the data. If no tests can be performed and no historical data are available, it might be possible to create a probability distribution using theoretical knowledge. If there is little knowledge available about the problem that is studied, then it might be necessary to use some general theoretical distribution, such as uniform, normal, triangular, etc. The character of the problem governs the type of distribution that will be selected. In this study the input parameters distribution is considered to be Gaussian distribution. Variation of parameters (standard deviation) is considered to be 10% on both sides of the mean for all the variables studied in this analysis.

B. Monte Carlo Simulation in ANSYS (Probability Design)

ANSYS provides two options for Monte Carlo simulations: the direct sampling method and the Latin hypercube sampling method.

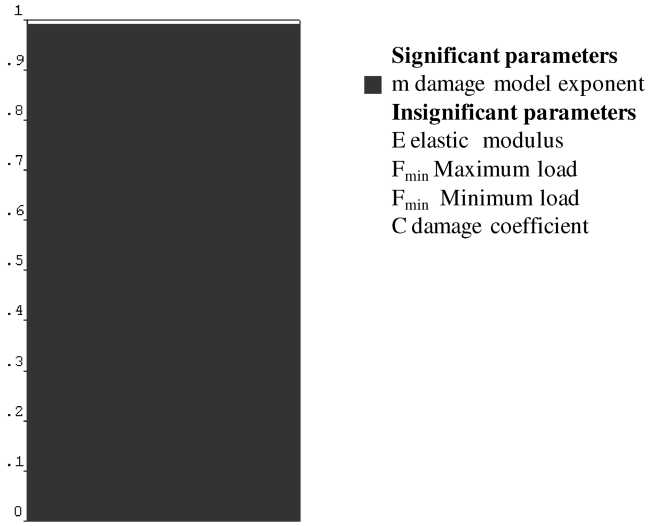

Fig. 12 Sensitivity analysis using the Monte Carlo simulation and varying material properties, load limits, and damage model constants.

The direct sampling method is the most commonly used form of the Monte Carlo analysis. It mimics natural processes that can be easily understood or imagined. However, it is not the most efficient technique. The fact that the sampling process has no "memory" means that there is a good chance that two samples can be selected from sampling points that occur extremely close together. In this event, no new information or insight into the behavior of a component will be gained by simulating two samples that are the same or very close to the same.

The second sampling method is the Latin hypercube sampling (LHS) method. The LHS is a more advanced and efficient technique differing only from the direct sampling method in that the sampling process has memory. This means that clustering of multiple samples is avoided and the tails of the distribution are forced to participate in the sampling. The LHS method typically requires 20–40% fewer simulation loops to deliver the same results with the same accuracy. Because of its advantages, LHS technique has been used in this study.

C. Sensitivity Results

The purpose behind performing a sensitivity analysis was to be able to identify which input variables in this study could affect the

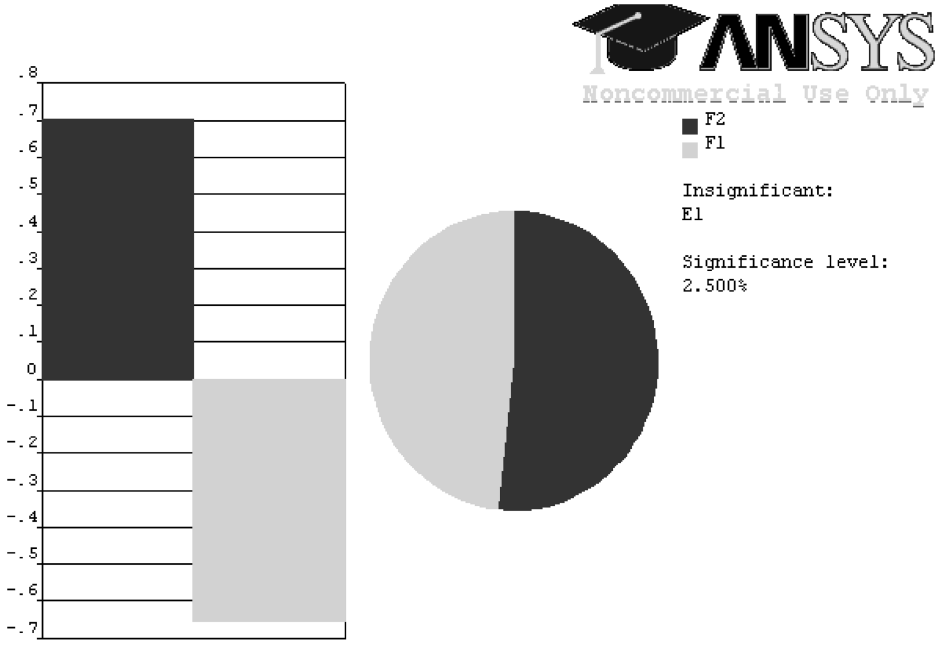

Fig. 13 Sensitivity analysis using Monte Carlo simulation and varying only material parameters and load limits.

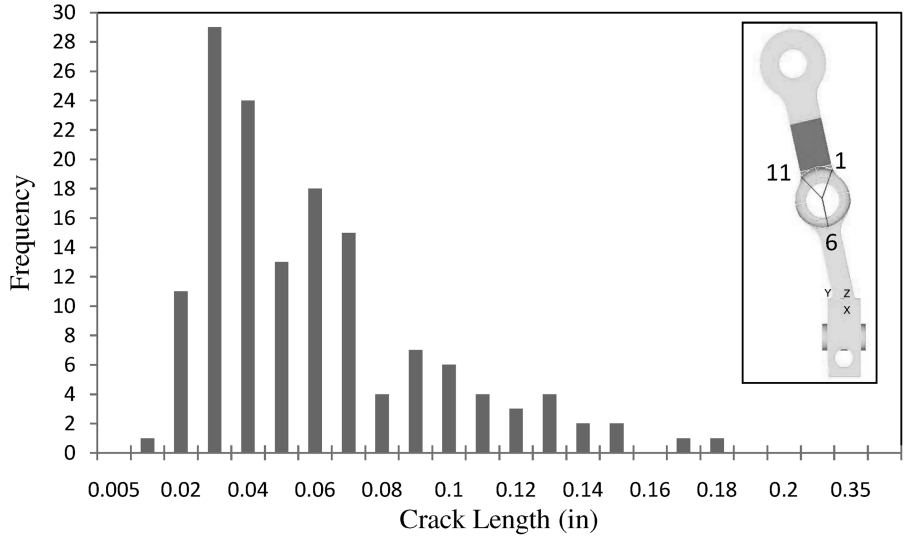

Fig. 14 The 11 o'clock position on the upper surface of the lever (courtesy of Hill Air Force Base Materials Laboratory).

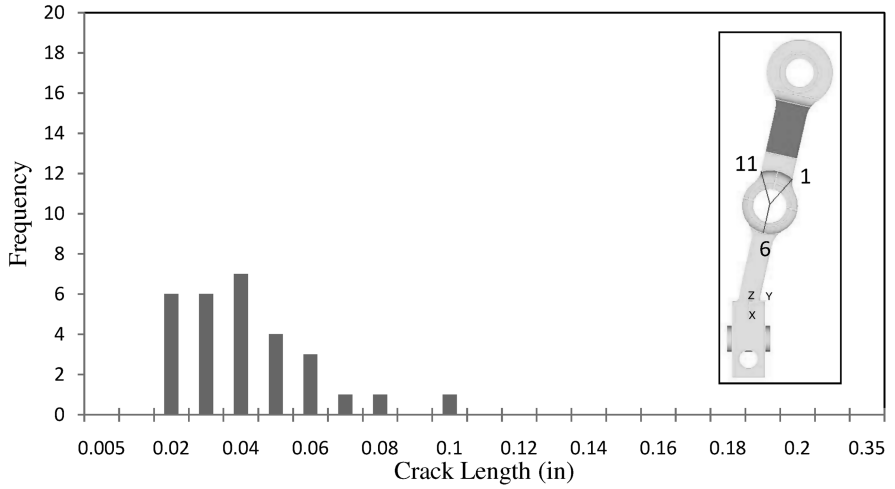

Fig. 15 The 11 o'clock position on the lower surface of the lever (courtesy of Hill Air Force Base Materials Laboratory).

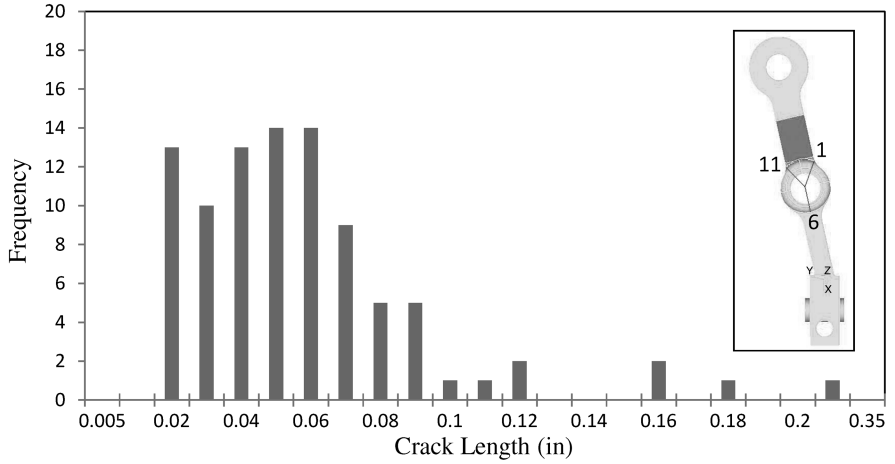

Fig. 16 The 1 o'clock position on the upper surface of the lever (courtesy of Hill Air Force Base Materials Laboratory).

initiation life of the lever. In the initial analysis, damage model parameters and the material properties and loads were varied in this sensitivity study. The results are shown in Fig. 12. This figure lists each of the input variables and gives the user a quick glance at which parameters significantly affect the initiation life of the lever. As was expected and is quite obvious from the data, only significant factor in the initiation life of the aileron lever is m, which is the exponent of the power-law equation for the fatigue model. The significance of other parameters is not comparable with this exponent. Therefore, the bar chart only consists of one shade, which indicates the impact of damage exponent. As clearly shown in this figure, the effect of exponent is so large that covers the effect of other parameters and shows as much as 99% effect.

Since this initial sensitivity analysis does not really show the effect of other parameters (in particular, the material properties and the load data), another analysis was conducted varying only the material

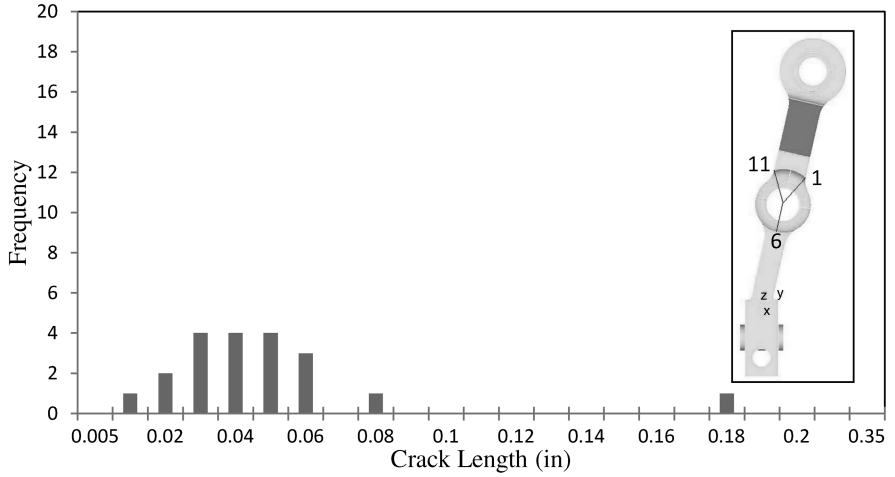

Fig. 17 The 1 o'clock position of the lower surface of the lever (courtesy of Hill Air Force Base Materials Laboratory).

properties and load limits. This analysis showed that significance of load variation is much higher than the material properties. The results are shown in Fig. 13.

VII. Results and Comparison with Field Data

Data of the location and lengths of the cracks found were provided by the Hill Air Force Base Materials Laboratory. The data were compiled from analyzing 275 levers using nondestructive investigation (NDI) techniques. From those levers, a total of 294 cracks were located and documented. Figures 14–17 show the approximate locations, number, and lengths for the majority of cracks detected. Additional cracks were located during the investigation; however, those additional cracks made up less than 1% of the total number of cracks discovered. For this reason, those locations have not been depicted in this study. It is evident from Fig. 10 that the majority of the damage and therefore the majority of the cracks were occurring at the 11 and 1 o'clock positions for both the upper and lower surfaces of the lever. This assertion is supported below by the evidence found in Figs. 14–17.

Analysis presented in this study compared with analysis done by Southwest Research Institute is more conservative in one way and is less conservative in another way. From one perspective, we are assuming that all the cycles have the maximum amplitude, but, in reality, it is not the case and the load cycles may have smaller amplitudes. In other words, most of the time, the lever goes through cycles that are much smaller than the cycle used in this analysis. So from this point of view, our approach is conservative. In another view, however, we assume that the lever is a perfect lever without any flaws or initial surface cracks, which may not always be true. Our analysis shows the crack initiation and propagation from undamaged perfect lever. However, fracture-mechanics-based approaches such as the one used at the Southwest Research Institute assume an initial crack and calculate the life assuming that initial flaw exists. So in that sense, the approach presented in this paper results in a longer life prediction and is not as conservative as a fracture-mechanics-based approach.

VIII. Conclusions

Following the catastrophic mishap of the T-38, an investigation was conducted to determine the cause of the mishap. Experimental data provided by Hill Air Force Base Materials Laboratory showed that the lever failed in a location uncommon to the remaining levers that were inspected using NDI techniques. The conflicting data had raised questions as to the locations and directions of crack growth. The current study stemmed from the uncertainty caused by the conflicting data and has shown that the majority of damage occurs on the lever at the 11 and 1 o'clock positions on both the upper and lower surfaces. These are the locations most susceptible to failure.

A finite element analysis model was produced using ANSYS. A Solid186 element was used during the meshing sequence for its exceptional ability to model irregular-shaped objects. A code was written that would draw, mesh, and apply forces for successive runs to the finite element analysis model. Using a continuum damage model coupled with a successive-initiation technique, damage to the individual elements was monitored. Using an appointed damage criteria, elements were killed, resulting in initiation sites and propagation paths of multiple cracks. The current research paper has shown the locations and propagation paths of cracks without presumption. Comparison of the experimental crack data has been shown to agree extremely well with the location of the cracks predicted by simulation.

Initiation and fatigue lives for the aileron lever were calculated as 1500 and 8600 h or 36,630 and 208,135 cycles, respectively. The crack propagation rate was calculated as 1.4693×10^{-7} in./cycle.

Acknowledgments

This work has been made possible by the support of the Mechanical Systems Engineering Branch at Hill Air Force Base, Utah. The author would also like to thank the Hill Air Force Base Materials Laboratory and Southwest Research Institute for the information provided through their reports.

References

[1] Schrader, K., Wieland, D., Burnside, H., Whitman, Z. L., Cronenberger, J., and Cardinal, J., "T-38 Aileron Actuator Servo Valve Lever Arm Engineering Evaluation," Ogden Air Logistics Center, Ogden, UT, 2008.

[2] Lemaitre, J., *A Course on Damage Mechanics*, Springer–Verlag, Berlin, 1992.

[3] Lemaitre, J., "A Continuous Damage Mechanics Model for Ductile Fracture," *Journal of Engineering Materials and Technology*, Vol. 107, 1985, pp. 83–89. doi:10.1115/1.3225775

[4] Chaboche, J. L., "Continuous Damage Mechanics—A Tool to Describe Phenomena Before Crack Initiation," *Nuclear Engineering and Design*, Vol. 64, 1981, pp. 233–247. doi:10.1016/0029-5493(81)90007-8

[5] Chaboche, J. L., "Continuum Damage Mechanics: Part I—General Concepts," *Journal of Applied Mechanics*, Vol. 55, 1988, pp. 59–64. doi:10.1115/1.3173661

[6] Chaboche, J. L., "Continuum Damage Mechanics: Part II—Damage Growth, Crack Initiation, and Crack Growth," *Journal of Applied Mechanics*, Vol. 55, 1988, pp. 65–71. doi:10.1115/1.3173662

[7] Kachanov, I. M., "Time of the Rupture Process Under Creep Conditions," *Izvestiya Akademii Nauk SSSR, Otdelenie Tekhnicheskikh Nauk*, No. 8, 1958, pp. 26–31.

[8] Frear, D. R., Jones, W. B., and Kinsman, K. R., "Solder Mechanics: A State of the Art Assessment," *First International Workshop on Materials and Mechanics Issues of Solder Alloy Applications*, Minerals, Metals & Material Society, Warrendale, PA, 1991.

[9] Basquin, O. H., "The Exponential Law of Endurance Tests," *Proceedings of the American Society for Testing and Materials*, Vol. 10, American Society for Testing and Materials, West Conshohocken, PA, 1910, pp. 625–630.

[10] Coffin, L. F., *Transactions of the ASME*, Vol. 76, 1954, pp. 931–950.

[11] Manson, S. S., *Experimental Mechanics*, Vol. 5, No. 4, 1965, pp. 193–226. doi:10.1007/BF02321056

[12] Hayden, H. W., Moffatt, W. G., and Wulff, J., *The Structure and Properties of Materials*, Vol. 3, Wiley, New York, 1965, p. 15.

[13] ANSYS Help, Element Reference, Element Library, V. 12.1.

[14] Okura, J. H., "Effect of Temperature and Moisture on Durability of Low Cost Flip Chip on Board (FCOB) Assemblies," Ph.D. Dissertation Defense, Department of Mechanical Engineering, University of Maryland, College Park, MD, 2001.

[15] Ladani, L. J., and Dasgupta, A., "Damage Initiation and Propagation in Voided Joints: Modeling and Experiment," *Journal of Electronic Packaging*, Vol. 130, No. 1, March 2008, Paper 011008. doi:10.1115/1.2837562

[16] Ladani, L. J., "Reliability Estimation for Large-Area Solder Joints Using Explicit Modeling of Damage," *IEEE Transactions on Device and Materials Reliability*, Vol. 8, No. 2, June 2008, pp. 375–386. doi:10.1109/TDMR.2008.919594

[17] Ladani, L. J., "Successive Softening and Cyclic Damage in Visco-Plastic Material," *Journal of Electronic Packaging*, Vol. 132, 2010, Paper 041011. doi:10.1115/1.4002722